




Research Article

Experimental measurement of thermal conductivity of stereolithography photopolymer resins

A. Oval-Trujillo¹  · A. Rodríguez^{1,2} · G. Pérez-Artieda^{1,2} · Y. Dung¹ · P. Alegría^{1,2}

Received: 15 March 2022 / Accepted: 20 June 2022

Published online: 08 July 2022

© The Author(s) 2022 

Abstract

The rise in the use of additive manufacturing highlights the importance of knowing the properties of the materials employed in this technology. Therefore, for the commercialization of thermal applications with this technology, heat management is essential. Here, computational modelling is often utilised to simulate heat transfer in various components, and knowing precisely the values of thermal conductivity is one of the key parameters. In this line of research, this paper includes the experimental study of three different types of resin used in additive manufacturing by stereolithography. Based on a test bench designed by researchers from the Public University of Navarre, which measures thermal contact resistances and thermal conductivities, the thermal conductivity analysis of three kinds of resin is carried out. This measuring machine employs the temperature difference between the faces and the heat flux that crosses the studied sample to determine the mentioned parameters. The thermal conductivity results are successful considering the constitution of the material studied and are consistent with the conductivity values for thermal insulating materials. The ELEGOO standard resin stands out among the others due to its low thermal conductivity of 0.366 W/m K.

Article Highlights

- Calculating thermal conductivity of three resins used in additive manufacturing by stereolithography.
- Contributing to a knowledge-based design of heat sink in thermal conductivity measurement bench.
- Improvement of the thermal conductivity measurement bench by reducing the uncertainty for its application in low thermal conductivity materials testing.

✉ A. Oval-Trujillo, anaterve.oval@unavarra.es | ¹Engineering Department, Public University of Navarre, Campus de Arrosadia s/n, 31006 Pamplona, Spain. ²Smart Cities Institute, 31006 Pamplona, Spain.



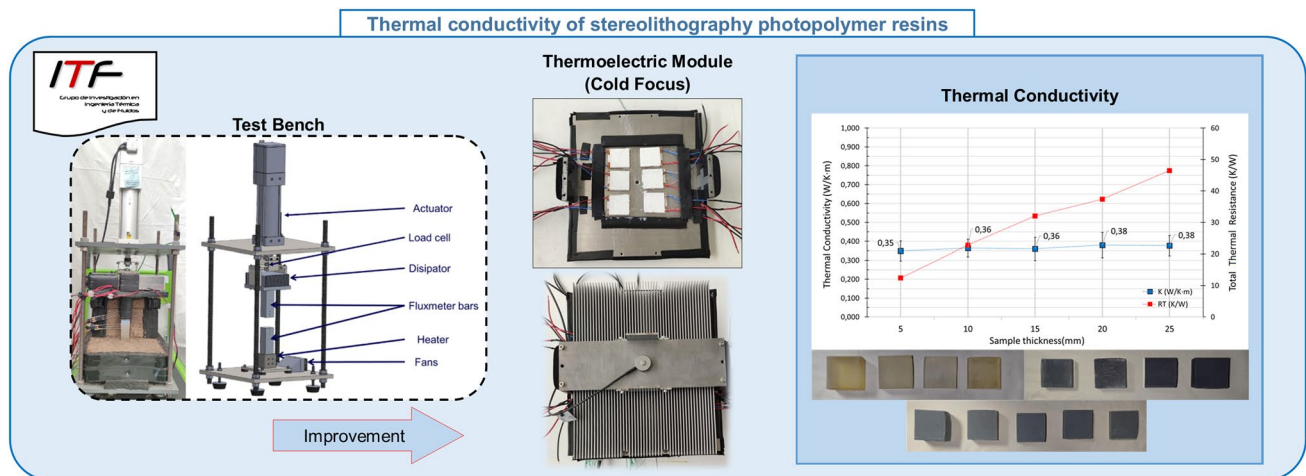
SN Applied Sciences

(2022) 4:205

| <https://doi.org/10.1007/s42452-022-05087-9>

SN Applied Sciences
A **SPRINGER NATURE** journal

Graphical abstract



Keywords Additive manufacturing · Stereolithography · Resin · Fused deposition modeling · Thermal conductivity · 3D printing

List of symbols

- T_i Temperature sensors in the fluxmeter "i = 1 to 6" (°C)
- SL Stereolithography
- FDM Fused deposition modeling
- TTR Total thermal resistance (K/W)
- TCR Thermal contact resistance (K/W)
- R_{TK} Conduction thermal resistance (K/W)
- Flux Fluxmeter
- $\dot{Q}_{F,Sup}$ Heat flow through the contact between fluxmeters (W)
- k Thermal conductivity (W/m K)
- k_e Average thermal conductivity of the sample of thickness e (W/m K)
- k_R Resin thermal conductivity (W/m K)
- X Sample thickness (m)
- A Cross-sectional area (m²)
- ΔT Temperature difference between the fluxmeter surfaces in contact with the sample
- L_i Sensors position in the fluxmeter "i = 1 to 4" (m)
- $T_{C,F,i}$ Temperature sensors in the fluxmeter, coldface. Sensors position in the fluxmeter L_4 (°C)
- $T_{C,C,i}$ Temperature sensors in the fluxmeter, hotface. Sensors position in the fluxmeter L_3 (°C)
- $T_{C,F,i+1}$ 10Min after, temperature sensors in the fluxmeter, coldface. Sensors position in the fluxmeter L_4 (°C)
- $T_{C,C,i+1}$ 10Min after, temperature sensors in the fluxmeter, hotface. Sensors position in the fluxmeter L_3 (°C)

- U_{ke} Uncertainty associated with each thickness (W/m K)
- U_k Uncertainty of the final value of the thermal conductivity (W/m K)

1 Introduction

Nowadays, manufacturing methods are in process of transformation due to new necessities pointing to goals like sustainability, personalization and adaptability. Additive manufacturing is a cutting-edge transformation, also known as 3D printing. These technologies are based on producing 3D items, applying material layer by layer with a final solidification of the raw material.

Stereolithography (SL) is a 3D printing technology used to manufacture pieces and models layer by layer. This method, which was patented by Hull [1], uses photopolymerization to obtain polymeric solid slabs. The stereolithography apparatus is a device that transforms a liquid polymer into a piece of solid polymer that generates the programmed object. This technique presents great precision and quality in the pieces. Other technologies present average roughness values (Ra) between 50 and 200 μ m. However, SL gets Ra values around 20 μ m [2]. The SL can be used in scales from very small objects of few millimeters, to pieces of decimeters [3].

One of the improvements proposed in the resins thermal conductivity for SL is the addition of nanofillers. Some authors have researched on the improvement of resin characteristics by the addition of nanofillers made of clays

or phyllosilicates, specifically halloysite (HNTs) [2]. They show an improvement of the conductivity of commercial SL resins. For example, Mubarak et al. [4] have studied the fillers made of silver particles coated with titanium nanoparticles (Ag-TNPs), whose results show the benefits of this technique. In their study, there are differences of conductivity as the nanofiller is added, concluding that the highest conductivity value is with a weight percentage of 1%. The silver molecules improve the thermal conduction, as silver is an excellent thermal conductor. However, the agglomeration of higher concentration of nanoparticles causes poor dispersion and improper cross-linking density. There are also references of the addition of aluminum particles to filaments used in additive fused wire deposition manufacturing (FDM) to improve thermal conductivity [5]. In this technology, the material from a wire coil is melted and deposited in layers, generating a geometry when the material solidifies. In the research, the highest value, that is 0.24 W/m K, is achieved by adding 25% aluminum to the samples.

Moreover, referring to additive manufacturing using fused deposition technology, some articles propose the inclusion of carbon fibers to improve thermal conductivity. Ibrahim et al. [6] analysed the variation of the conductivity of a nylon matrix sample, with different layer configurations and fiber directions, obtaining the maximum conductivity with fibers in the direction of the heat flow and reaching a conductivity 11 times higher than that of the base material.

In the case of post-processing, like sintering of materials with copper particles, the thermal conductivity can be strongly increased, as Dehdari et al. [7] analysed. Starting

with a material whose average volume content is 39.3% and whose conductivity is 1.5 W/m K, they increased the copper concentration to 42.3% and reduced the porosity by sintering, obtaining a conductivity of 25.5 W/m K. In conclusion, their study showed the different applications of this technique, only adding different materials at the nanometer scale on the same base or matrix.

On the other hand, referring to the test bench, the methods for measuring thermal conductivity of solid materials can be divided into two categories; steady-state methods and transient or non-steady-state methods [8–13]. Some of these methods have been used to measure the thermal conductivity of materials used in additive manufacturing, both transient methods [13, 14] and steady-state methods [15–17].

The steady state meter bar method used in this article has been widely used to measure the thermal conductivity of solid materials. The methodology used in these devices is based on an implementation of the ASTM D5470 Standard, where the sample is placed between two instrumented meter bars (fluxmeter) to measure the heat flow through the sample and the temperature drop between the surfaces in contact. From these measurements, the thermal conductivity of the sample can be determined.

Therefore, due to the lack of information about thermal conductivity of additive manufacturing by stereolithography material and the possible application of these materials in heatsink elements, this article aims to cover the experimental study of the thermal conductivity of different resins used in SL. The work is organized as follows: in the following section, we introduce a description of the test bench used, the study samples and the thermal

Fig. 1 Thermal conductivity measurement bench



characterization method. In Sect. 3, we show the uncertainty calculations. Then, in Sect. 4, we present the results of thermal conductivity according to the expressions presented in previous sections. Finally, Sect. 5 draws the conclusions and shows directions for future work.

2 Material and method

2.1 Test bench

The test bench used to measure thermal conductivity operates in steady-state. It is based on the generation of an unidirectional heat flow and the temperature difference of the sample studied, which will be a function of the thermal conductivity. In the ITF (Thermal and Fluid Engineering—Ingeniería Térmica y de Fluidos) research group, thermal conductivity studies have already been carried out using this test bench of their own design and manufacture [18].

A photograph of the test bench and a schematic representation of its elements are shown in Fig. 1. The structure (sandwich type) of the test bench has the following elements, from bottom to top:

A calibrated electrical resistance provides a heat flow (an external energy source). The first fluxmeter (bottom fluxmeter) transmits the heat to the sample, which is also in contact with the top fluxmeter. This one transmits the heat flow to a cooling system, consisting of a finned heat sink and four fans (forced convection). Finally, the cold set is assembled using four screws that connect the heatsink

to a rigid base. In order to control the pressure on the sample, a combination of a linear actuator and a structure, which moves the assembly in a guided way, is used. The test bench has pressure and temperature sensors.

The heat flux conduction through the studied sample must be unidirectional, so there are two fluxmeters of a conductive material (304 AISI INOX) that are well insulated on the sides as shown in Fig. 2. Likewise, each fluxmeter has three Pt-100 temperature sensors (model FPA15L0100, with a measuring range from -50 to 500 °C, an uncertainty of 0.1 °C, and a diameter of 1.5 mm). The temperature sensors are inserted in holes made on the fluxmeters, which present a depth of 20 mm (Fig. 2). An additional sensor measures the ambient temperature and the heat sink temperature. The uncertainties associated to the temperatures, lengths and diameters were calculated in the calibration laboratory Applus + AC6, located in Navarra (Spain).

With the temperature data of the sensors, one can extrapolate and know the temperature of the contact faces between the fluxmeters and the sample. Since the heat flux, obtained from the gradient and the thermal conductivity of the fluxmeters, is known, the contact thermal resistance, total thermal resistance and thermal conductivity of the sample material can be determined. For the heat flow through the test pieces to be the same, they must have the same contact area, 40×40 mm², and their thickness is variable in order to compare and to obtain the calculation parameters.

To register data, the sample is placed between the upper and the lower fluxmeter, a pressure is applied on the sample (the same for all tests), it is insulated, and the hot

Fig. 2 Sample and temperature sensors [18]

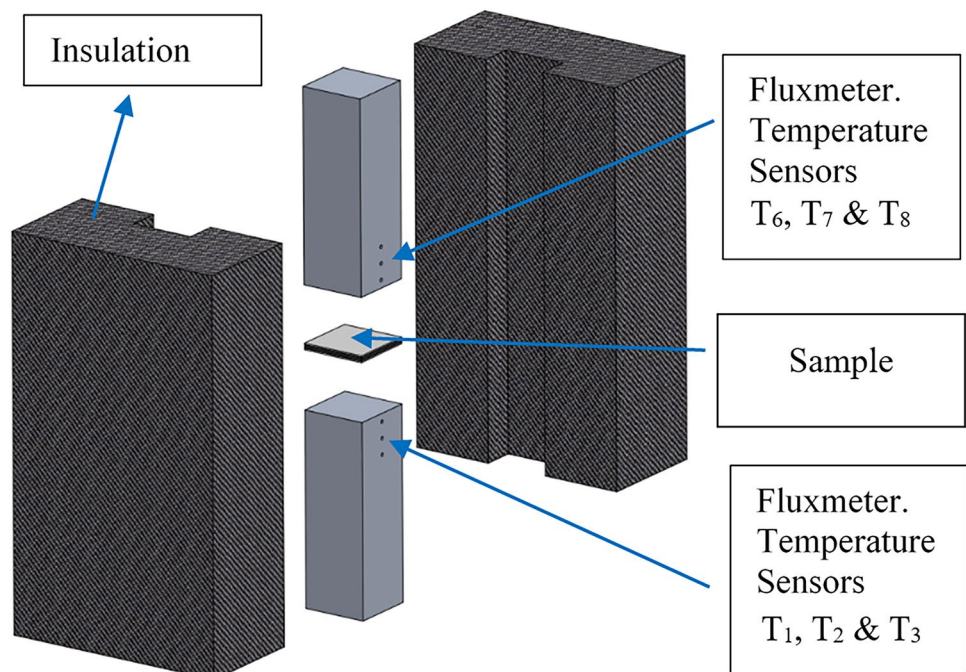
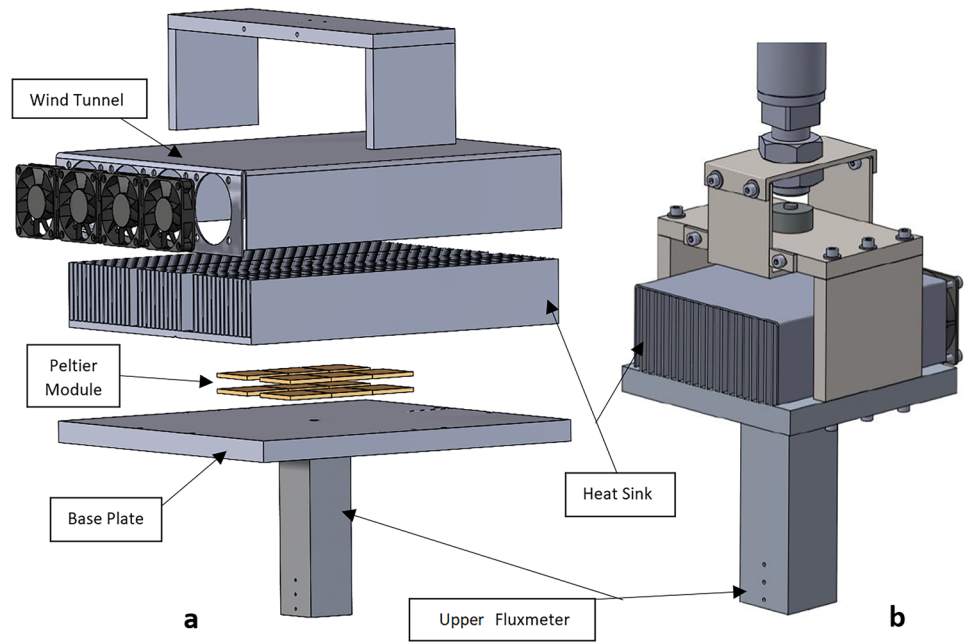


Fig. 3 Comparison of the original bench and the modification. From left to right **a** modification, **b** original



sink is heated (always supplying, for each test, the same power). The temperature measurements were recorded in the ALMEMO 5690-2M09TG3 connected to a computer.

2.1.1 Improvement of the test bench for the study of samples with low thermal conductivity

Some improvements have been applied to the bench described in the article by Rodríguez et al. [18]. Since the bench was designed to measure relatively high conductivities (steel, aluminium, etc.) and the materials under study are now insulated and present higher thermal resistance, it is necessary to achieve a greater temperature gradient between adjacent Pt-100 sensors.

For this goal, a multistage disposition of Peltier modules (TG12-8-01L) is used as a cooling system to improve the capacity of the cold source. The purpose is to generate a heat flow that extracts energy from the system and reduces the cold sink temperature. Likewise, the hot side of the modules is cooled by forced convection through a finned heatsink (Fig. 3).

With this system, a greater temperature gradient is achieved between the sounding lines of both fluxmeters, increasing the temperature difference between adjacent temperature sensors from 0.3 to 2.5 °C. Consequently, the bench's uncertainty for testing materials is reduced with low thermal conductivity. The cold side temperature has been reduced from 20 to – 5 °C (in an ambient

temperature of 18 °C), obtaining an improvement of 25 °C. Thus, the bench is ready for the study of the insulating materials presented in this article.

Once the test has stabilised according to the established criterion of stability, the results are extracted for post-processing.

2.1.2 Stability criterion

To consider that the test has stabilised, it is established as a criterion that the temperature difference, ΔT_{3-6} , between the sensor closest to the cold side of the sample, T3, and the one closest to the hot side of the sample, T6, during a time interval of 10 min varies by less than 0.5 °C (Fig. 4).

$$\text{Stabilitycriterion} = \Delta T = \Delta T_{3-6,i+1} - \Delta T_{3-6,i} \quad (1)$$

In order to compare samples of the same thickness, and to be able to calculate the thermal contact resistance, the samples shall be tested three times under the same conditions of power in the sinks and pressure.

2.2 Study samples

The manufacture of the studied pieces has been carried out by SL 3D printing, using three different sorts of resins. On the one hand, High Temp resin from Formlabs, which has mechanical characteristics of 58.3 MPa of yield strength and 2.75GPa of elasticity modulus. In terms of the thermal properties of the material, according to the

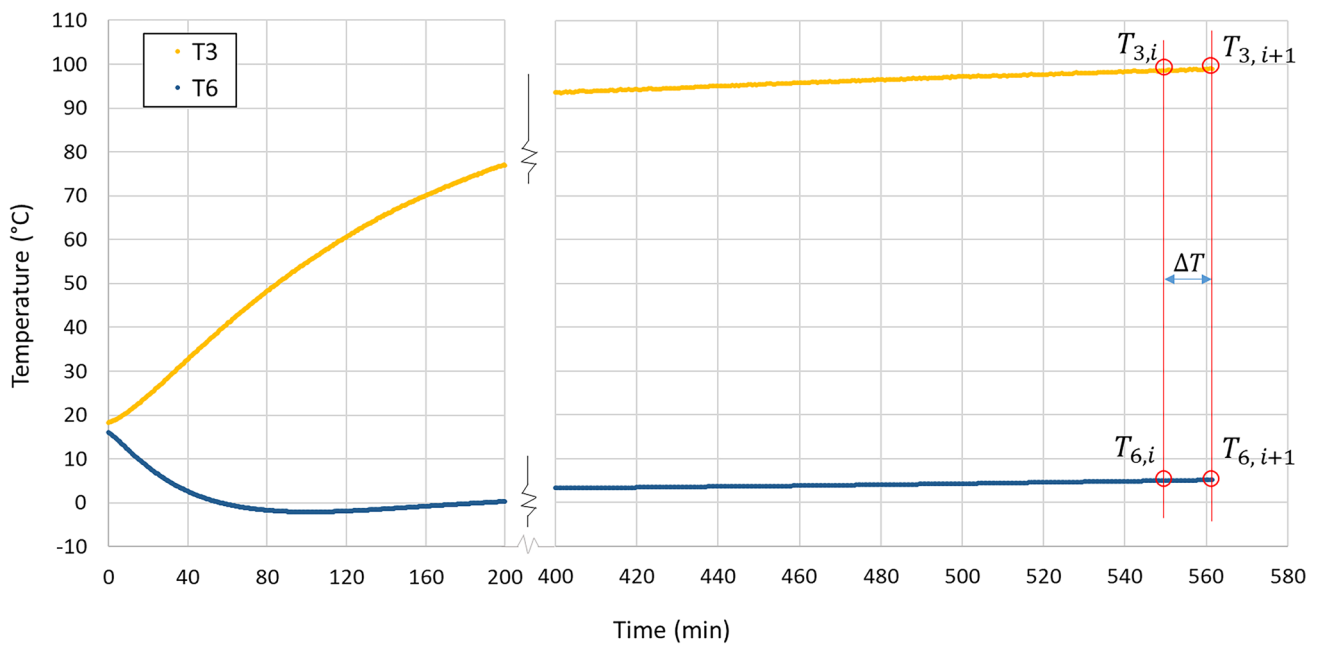


Fig. 4 Stability condition

Table 1 Study samples

Thermal conductivity study samples							
Sample	Material	Size				Average roughness (μm)	
			Thickness (mm)	Width (mm)	Length (mm)	Underside	Top face
Sample 1	HIGH TEMP	5.10		40.50	40.00	1.602	1.138
Sample 2	HIGH TEMP	10.10		40.00	40.00	1.690	0.321
Sample 3	HIGH TEMP	20.10		40.00	40.00	3.057	2.999
Sample 4	HIGH TEMP	25.00		40.50	40.00	4.876	2.715
Sample 5	RES-WASHABLE	5.20		40.50	40.00	1.320	0.906
Sample 6	RES-WASHABLE	10.20		40.70	40.00	1.656	0.816
Sample 7	RES-WASHABLE	15.20		40.65	40.00	2.306	1.109
Sample 8	RES-WASHABLE	20.10		40.40	40.00	3.667	1.384
Sample 9	RES-WASHABLE	25.00		40.55	40.00	2.346	1.564
Sample 10	RES-STANDARD	5.20		40.60	40.00	2.496	0.741
Sample 11	RES-STANDARD	10.20		40.90	40.00	3.271	1.482
Sample 12	RES-STANDARD	15.30		40.70	40.00	4.531	0.862
Sample 13	RES-STANDARD	20.10		40.70	40.00	4.022	0.738
Sample 14	RES-STANDARD	25.15		40.70	40.00	3.233	1.909

manufacturer, the temperature of thermal deflection at a pressure of 0.45 MPa is 142 °C. The tests were carried out by applying a pressure of 0.42 MPa.

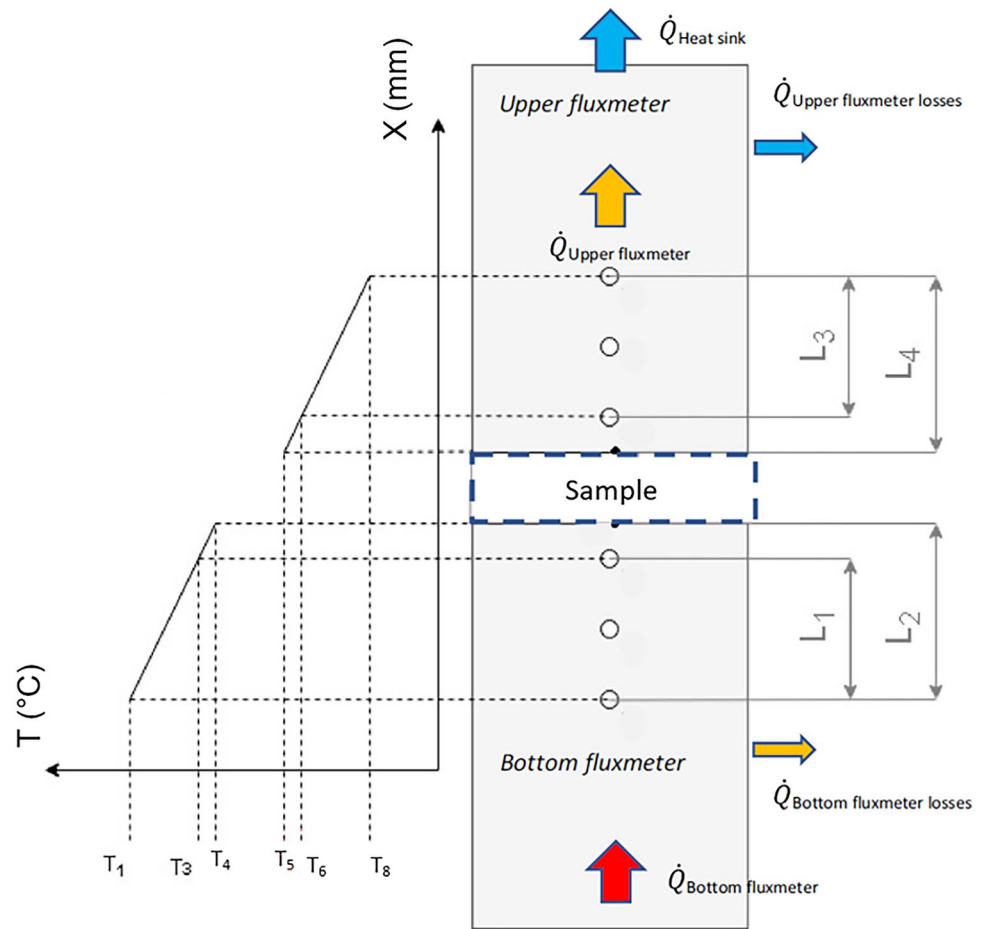
Regarding the two other materials, these are Water Washable Resin and Standard Resin, both from the manufacturer ELEGOO. Unlike the High Temp resin, the thermal characteristics of these are not specified, except the maximum temperature they withstand, which is 80 °C. For this reason, the studies made on the Washable and Standard

resin samples control this maximum temperature, also setting a working pressure of 0.42 MPa (as it is done for the Formlabs resin studies).

2.2.1 Geometry

Square samples are tested, with a dimensional standard of 40 × 40 mm² contact area and different thicknesses. The

Fig. 5 Distance between thermocouples and temperature drop in sample



roughness of each of the samples faces in contact with the fluxmeters was also measured (Table 1).

2.3 Thermal characterization method

For the analysis of the results of the different studies, once the temperatures corresponding to each experimental point are determined (Fig. 5), the next steps are carried out:

- (1) The recorded temperature is adjusted according to the calibration of the temperature sensors (T₁, T₃, T₆ and T₈). These calibration adjustments were made, before starting the study shown in this article, in the calibration laboratory Applus + AC6.
- (2) The extrapolated temperatures of the top and bottom faces of the sample (T₄ and T₅) are determined using Eqs. (2 and 3).

$$T_4 = \frac{L_2}{L_1} \times T_3 + \left(1 - \frac{L_2}{L_1}\right) \times T_1 \quad [^\circ\text{C}] \quad (2)$$

$$T_5 = \frac{L_4}{L_3} \times T_6 + \left(1 - \frac{L_4}{L_3}\right) \times T_8 \quad [^\circ\text{C}] \quad (3)$$

- (3) The heat flux through the upper fluxmeter is calculated, using the temperature values of the sensors and the thermal conductivity of the fluxmeter, Eq. (4) [19].

$$\dot{Q}_{F.Sup} = A_{Flux} \times k_{Flux} \times \frac{T_6 - T_8}{L_3} \quad [\text{W}] \quad (4)$$

- (4) The Total Thermal Resistance (TTRi) can be determined from the heat flux calculated in the previous step and the surface temperatures of the sample, Eq. (5). Also, the TTRi is composed of the contact resistance between the sample face and the fluxmeter (TCR) and the resistance due to the thermal conductivity of the sample (k), as expressed in Eq. (6).

$$TTRi = \frac{T_4 - T_5}{\dot{Q}_{F.Sup}} \quad [\text{K/W}] \quad (5)$$

(5) To calculate the Thermal Conductivity of the Material, k , a comparison is made between the results of the total thermal resistance (TTRi) of two samples of different thicknesses, obtaining a system of 2 equations and 2 unknowns (TCR and k), Eq. (7).

$$TCR = \frac{TTR_i - \frac{X_i}{kA_i}}{2} = \frac{TTR_j - \frac{X_j}{kA_j}}{2} \tag{7}$$

$$k_i = \frac{\frac{X_j}{A_j} - \frac{X_i}{A_i}}{TTR_j - TTR_i} \quad [W/mK] \tag{8}$$

Since the test procedure is repetitive, as it is always performed under the same pressure level, the same type of thermal paste and the same way of applying the thermal paste in order to reduce the roughness contribution of the samples and to improve the thermal contact, it is considered that the thermal contact resistance (TCR) will remain constant.

$$TTR_i = 2 \times TCR + R_{k-sample,i} = 2 \times TCR + \frac{X_i}{kA_i} \tag{6}$$

2.3.1 Bullet "i" and "j" stand for studies of samples of different thicknesses

After obtaining the value of k , the thermal contact resistance can be calculated.

Fig. 6 Study result. Resin Type 1- HIGH TEMP [sample contact area $40 \times 40 \text{ mm}^2$]

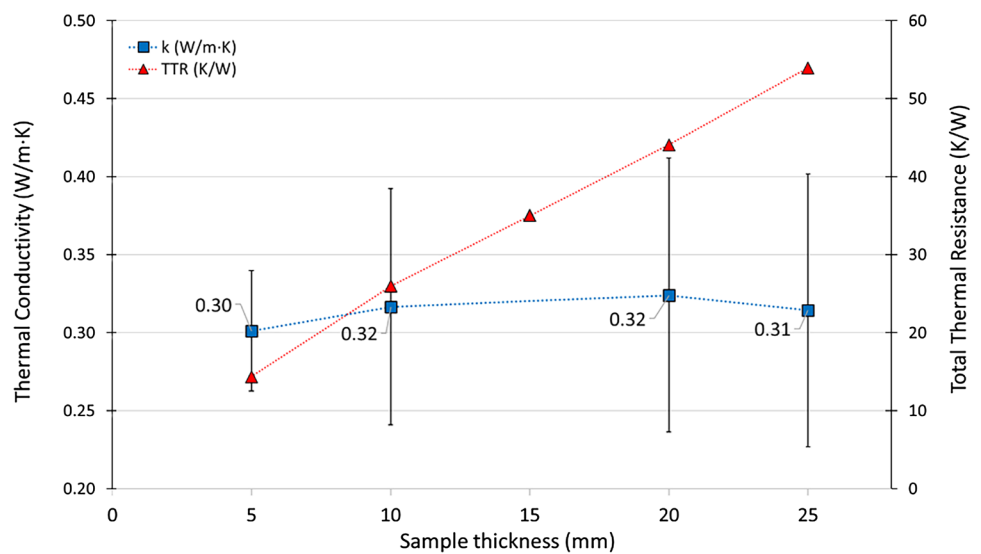


Fig. 7 Study result. Resin Type 2- WASHABLE [sample contact area $40 \times 40 \text{ mm}^2$]

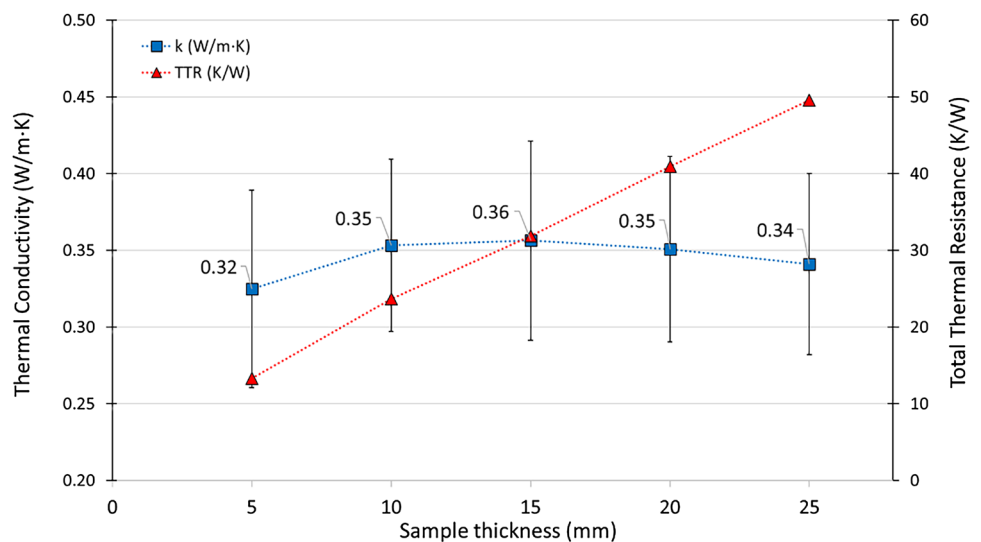


Fig. 8 Study result. Resin Type 3- STANDARD [sample contact area 40 × 40 mm²]

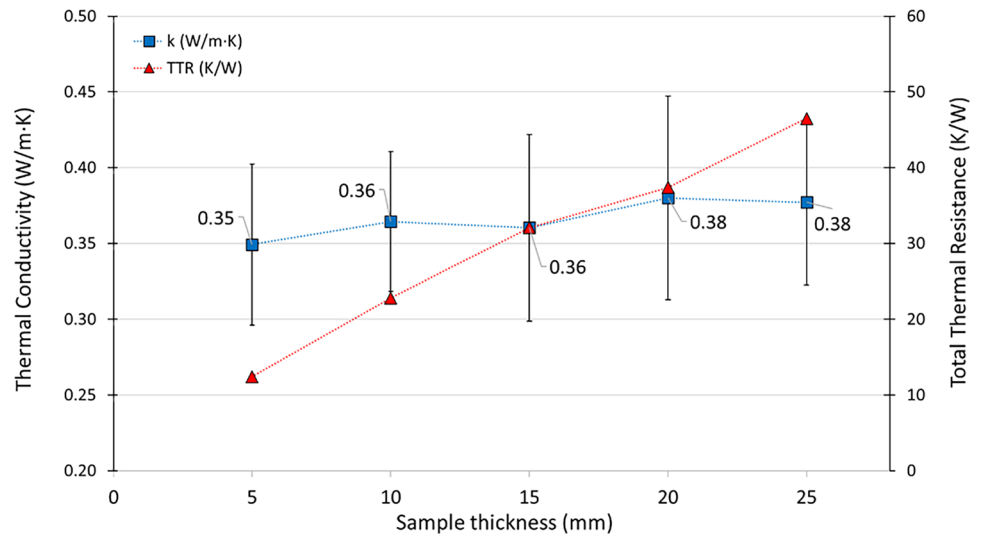


Table 2 Thermal conductivity of each material

	Resin 1 "High Temp"[Formlab]	Resin 2 "Washable"[ELEGOO]	Resin 3 "Standard"[ELEGOO]
k (W/m K)	0.314	0.343	0.366
Uncertainty	±0.087	±0.061	±0.056

$$TCRi = \frac{TTRi - \frac{X_i}{k_i A_i}}{2} \quad [K/W] \quad (9)$$

Three tests were carried out on each thickness (5, 10, 15, 15, 20, 25 mm), calculating with the methodology described above both the total thermal resistance and the thermal conductivity at each thickness, k_e (average of all their relationships), as shown in Figs. 6, 7 and 8.

The thermal conductivity of the material is the average of these k_i figures obtained for each ratio (Table 2).

$$k = \frac{\sum_e k_e}{5} \quad [W/mK] \quad (10)$$

3 Uncertainty

Uncertainty is composed of random uncertainty on the one hand, and systematic uncertainty on the other. For the uncertainty study described in this article, the contribution of the random uncertainty is disregarded, as the high number of repetitions (relationships) means that the figure of this uncertainty is several orders of magnitude lower than the systematic uncertainty ($\times 10^{-5}$). The position of the probes has been measured with high accuracy and its contribution to the measurement uncertainty is less than 0.1%. Therefore, to simplify the uncertainty calculation, it

is assumed that the length values of the probe positions do not contribute to the uncertainty calculation.

As science references, for the calculation of the uncertainty [20], thermal conductivity should be obtained employing the expressions. Using equations (Eqs. 2–5), the general expression of the total thermal resistance is obtained as a function of the sensors measurements:

$$TTRi = \frac{\left[\frac{L2}{L1} T3 + \left(1 - \frac{L2}{L1} \right) T1 \right] - \left[\frac{L4}{L3} T6 + \left(1 - \frac{L4}{L3} \right) T8 \right]}{A_{Flux} k_{Flux} \frac{T6-T8}{L3}} \quad [K/W] \quad (11)$$

The uncertainty associated with the thermal resistance calculation is determined from the derivatives of the general expression and the uncertainty figures of the sensors calculated in the calibration laboratory Applus + AC6 ($b_{T1}^2 = 0.043, b_{T3}^2 = 0.045, b_{T6}^2 = 0.044, b_{T8}^2 = 0.044$).

$$b_{TTRi}^2 = \left(\frac{\partial}{\partial T1} \right)^2 \times b_{T1}^2 + \left(\frac{\partial}{\partial T3} \right)^2 \times b_{T3}^2 + \left(\frac{\partial}{\partial T6} \right)^2 \times b_{T6}^2 + \left(\frac{\partial}{\partial T8} \right)^2 \times b_{T8}^2 \quad (12)$$

b_{TTRi}^2 is calculated for each test performed. For each study, an uncertainty associated with the calculation of the thermal resistance is calculated as a function of the temperature (T1, T3, T6, T8) recorded for each case.

Similarly to the process carried out for the calculation of the uncertainty of the total thermal resistance, the systematic uncertainty associated with the calculation of the thermal conductivity as a function of thickness is determined from the expression of the thermal conductivity, (Eq. 8).

$$b_{ki}^2 = \left(\frac{\partial}{\partial TTR_j} \right)^2 \times b_{TTR_j}^2 + \left(\frac{\partial}{\partial TTR_i} \right)^2 \times b_{TTR_i}^2 \quad (13)$$

b_{ki}^2 is calculated for each relationship used for the calculation of the thermal conductivity. For each one, an uncertainty associated with the calculation of the conductivity is calculated as a function of the thermal resistance. This last is already calculated according to expression (Eq. 5), and its uncertainty is obtained from equation (Eq. 12).

Therefore, the uncertainty associated with each thickness is calculated by substituting in the expression of the total uncertainty, U_{ke} , the largest figures of b_{ki}^2 , differentiating between thicknesses, b_{kei}^2 .

$$U_{ke} = 2 \times \sqrt{b_{kei}^2} \quad (14)$$

About the uncertainty the final thermal conductivity value of the material under study, U_k , it is proceeded in the same way but without differentiating between thicknesses, the highest cipher among all the systematic uncertainties obtained is taken, the highest figure b_{ki}^2 obtained in Eq. (13).

$$U_k = 2 \times \sqrt{b_{ki}^2} \quad (15)$$

4 Results

Based on the conductivity results calculated according to the expressions in the methodology section, the values obtained for each of the thicknesses studied are averaged. These values for each material are shown in the final table (Table 2).

As shown in the graphic, low thermal conductivity values are obtained for all resin types as expected for mainly thermal insulating materials, although there are significant differences between them. In heat dissipation applications, the main material used is aluminum alloy. Its conductivity value is around 160 W/m K even three orders of magnitude lower in all cases.

With regard to the comparison of the results of the resins, the repeatability of the test set and the linearity of the values obtained according to the proposed method stand out. It has been obtained that Standard (ELEGOO) resin (third), whose thermal conductivity value is 0.366 ± 0.056 W/m K, relatively higher than the others.

However, it does not have the same benefits, such as the high heat resistance of the first resin or the washable resin characteristic of the second one. For these two resins, their conductivities are 0.314 ± 0.087 W/m K (Resin 1 [High Temp]) and 0.343 ± 0.061 W/m K (Resin 2 [Washable]). In addition, taking into account that the measurement uncertainty is between 20 and 30% of the value, and that the difference between the results of the resins is of 10%, it is concluded that the values obtained are similar.

The results shown in the G. Hu et al. [2] article, present similar values with results of 0.574 W/m K compared to the thermal conductivity of 0.366 W/m K obtained in our study. Nonetheless, it should be taken into account that these are studies in which nanofibers have been introduced into the materials to increase their thermal conductivity and it is logical that this value extracted from the literature corresponds to an addition of 3% Cu in the composition of the resin. Furthermore, the resins thermal conductivity is similar but higher than commercial additivated filaments ones with 25% Al additives, which is of 0.24 W/m K, as published in the article by Melchels et al. [5].

5 Conclusions

The main conclusions drawn from this research are: First, the thermal conductivity measurement bench of the ITF group has been adapted to measure materials with low thermal conductance. For this purpose, the heat sink has been improved with a thermoelectric cooling system achieving a reduction of the temperature of the fluxmeter higher than 25 °C. This new measurement bench gives linearity in the results as well as repeatability of the tests. The modification allows maintaining a stable heat flux in each test, which is largely unaffected by ambient conditions. The introduction of a cold sink at sub-zero temperatures, implemented in the modified thermal conductivity measurement bench, reduces the uncertainty and increases the stability and repeatability of the tests. The maximum uncertainty value obtained is ± 0.087 W/m K.

On the other hand, three different types of resins manufactured by SL have been measured, obtaining similar values among them, and similar to those reported in the literature shown in this article. The highest thermal conductivity value is obtained for the standard resin, which is 0.366 ± 0.056 W/m K. As expected, this thermal conductivity value is lower than the values of the resins thermally doped with nanoparticles, conductivities around 0.600 W/m K for the resins [4], and 0.24 W/m K for the Al-additivated filaments [5].

Therefore, the improvements introduced have widened the application range of our bench, which will allow us to

study new materials to select the optimal ones from the thermal point of view in different applications. In addition, although the results with the heat sink with thermoelectric cooling are acceptable, as future lines of research we will study new cooling systems with vapor compression coolers and water heat exchangers, to check if it is possible to obtain lower uncertainty values.

Acknowledgements The authors are indebted to the Department of Economic and Business Development of Navarre Government, for economic support to this work, included in R&D projects in 2020: FORM3D 0011-1365-2020-000084 research project.

Funding The authors have not disclosed any funding.

Declarations

Conflict of interest The authors declare that they have no conflict of interest.

Open Access This article is licensed under a Creative Commons Attribution 4.0 International License, which permits use, sharing, adaptation, distribution and reproduction in any medium or format, as long as you give appropriate credit to the original author(s) and the source, provide a link to the Creative Commons licence, and indicate if changes were made. The images or other third party material in this article are included in the article's Creative Commons licence, unless indicated otherwise in a credit line to the material. If material is not included in the article's Creative Commons licence and your intended use is not permitted by statutory regulation or exceeds the permitted use, you will need to obtain permission directly from the copyright holder. To view a copy of this licence, visit <http://creativecommons.org/licenses/by/4.0/>.

References

- Hull CW (1986) U.S. Patent 4,575,330. Apparatus for Production of Three-Dimensional Objects by Stereolithography
- Hu G, Cao Z, Hopkins M, Lyons JG, Brennan-Fournet M, Devine DM (2019) Nanofillers can be used to enhance the thermal conductivity of commercially available SLA resins. *Procedia Manuf* 38:1236–1243. <https://doi.org/10.1016/j.promfg.2020.01.215>
- Melchels FPW, Feijen J, Grijpma DW (2010) A review on stereolithography and its applications in biomedical engineering. *Biomaterials* 31(24):6121–6130. <https://doi.org/10.1016/j.biomaterials.2010.04.050>
- Mubarak S et al (2020) A novel approach to enhance mechanical and thermal properties of SLA 3D printed structure by incorporation of metal-metal oxide nanoparticles. *Nanomaterials* 10(2):217. <https://doi.org/10.3390/nano10020217>
- Relinque JJ, Romero-Ocaña I, Navas-Martos FJ, Delgado FJ, Domínguez M, Molina SI (2020) Synthesis and characterisation of acrylic resin-al powder composites suitable for additive manufacturing. *Polymer* 12(8):1642. <https://doi.org/10.3390/polym12081642>
- Ibrahim Y, Elkholy A, Schofield JS, Melenka GW, Kempers R (2020) Effective thermal conductivity of 3D-printed continuous fiber polymer composites. *Adv Manuf Polym Compos Sci* 6(1):17–28. <https://doi.org/10.1080/20550340.2019.1710023>
- Dehdari Ebrahimi N, Ju YS (2018) Thermal conductivity of sintered copper samples prepared using 3D printing-compatible polymer composite filaments. *Addit Manuf* 24:479–485. <https://doi.org/10.1016/j.addma>
- Zhao D, Qian X, Gu X, Ayub Jajja S, Yang R (2016) Measurement techniques for thermal conductivity and interfacial thermal conductance of bulk and thin film materials. *J Electron Packag* 138:040802. <https://doi.org/10.1115/1.4034605>
- Adamczyk WP, Pawlak S, Ostrowski Z (2018) Determination of thermal conductivity of CFRP composite materials using unconventional laser flash technique. *Meas J Int Meas Confed* 124:147–155. <https://doi.org/10.1016/j.measurement.2018.04.022>
- Aksöz S, Öztürk E, Maraşlı N (2013) The measurement of thermal conductivity variation with temperature for solid materials. *Meas J Int Meas Confed* 46(1):161–170. <https://doi.org/10.1016/j.measurement.2012.06.003>
- Kempers R, Kolodner P, Lyons A (2009) A high-precision apparatus for the characterization of thermal interface materials. *Rev Sci Instrum* 80:95111. <https://doi.org/10.1063/1.3193715>
- Adamczyk WP, Białecki RA, Kruczek T (2017) Measuring thermal conductivity tensor of orthotropic solid bodies. *Meas J Int Meas Confed* 101:93–102. <https://doi.org/10.1016/j.measurement.2017.01.023>
- Shemelya C et al (2017) Anisotropy of thermal conductivity in 3D printed polymer matrix composites for space based cube satellites. *Addit Manuf* 16:186–196. <https://doi.org/10.1016/j.addma.2017.05.012>
- Guo R, Ren Z, Bi H, Xu M, Cai L (2019) Electrical and thermal conductivity of polylactic acid (PLA)-based biocomposites by incorporation of nano-graphite fabricated with fused deposition modeling. *Polymer* 11:3. <https://doi.org/10.3390/polym11030549>
- Prajapati H, Ravoori D, Woods RL, Jain A (2018) Measurement of anisotropic thermal conductivity and inter-layer thermal contact resistance in polymer fused deposition modeling (FDM). *Addit Manuf* 21:84–90. <https://doi.org/10.1016/j.addma.2018.02.019>
- Flaata T, Michna GJ, Letcher T (2017) Thermal conductivity testing apparatus for 3D printed materials. *ASME 2017 Heat Transfer Summer Conference* 2. Paper No: HT2017–4856, V002T15A006, p. 6. <https://doi.org/10.1115/HT2017-4856>
- Laureto J, Tomasi J, King JA, Pearce JM (2017) Thermal properties of 3-D printed polylactic acid-metal composites. *Prog Addit Manuf* 2(1–2):57–71. <https://doi.org/10.1007/s40964-017-0019-x>
- Rodríguez A, Pérez-Artieda G, Beisti I, Astrain D, Martínez A (2020) Influence of temperature and aging on the thermal contact resistance in thermoelectric devices. *J Electron Mater* 49(5):2943–2953. <https://doi.org/10.1007/s11664-020-08015-y>
- Çengel YA, Ghajar AJ, Muñoz Díaz E (2020) *Transferencia de calor y masa: fundamentos y aplicaciones*. McGraw-Hill/Interamericana Editorial, Guaynabo
- Coleman HW, Steele WG (2018) *Answers to selected problems, experimentation, validation and uncertainty analysis for engineers*. Wiley, Hoboken, NJ

Publisher's Note Springer Nature remains neutral with regard to jurisdictional claims in published maps and institutional affiliations.